

Temporal Incoherence Induced Upon a High- Intensity Beam by Plasma Propagation

J. Fuchs, C. Labaune, S. Depierreux, H. Bandulet, P. Michel, H. A. Baldis

*This article was submitted to the **Second International Conference on Inertial Fusion Sciences and Applications (IFSA 2001)**, Kyoto, Japan, September 9-14, 2001*

September 25, 2001

U.S. Department of Energy

Lawrence
Livermore
National
Laboratory

DISCLAIMER

This document was prepared as an account of work sponsored by an agency of the United States Government. Neither the United States Government nor the University of California nor any of their employees, makes any warranty, express or implied, or assumes any legal liability or responsibility for the accuracy, completeness, or usefulness of any information, apparatus, product, or process disclosed, or represents that its use would not infringe privately owned rights. Reference herein to any specific commercial product, process, or service by trade name, trademark, manufacturer, or otherwise, does not necessarily constitute or imply its endorsement, recommendation, or favoring by the United States Government or the University of California. The views and opinions of authors expressed herein do not necessarily state or reflect those of the United States Government or the University of California, and shall not be used for advertising or product endorsement purposes.

This is a preprint of a paper intended for publication in a journal or proceedings. Since changes may be made before publication, this preprint is made available with the understanding that it will not be cited or reproduced without the permission of the author.

This work was performed under the auspices of the United States Department of Energy by the University of California, Lawrence Livermore National Laboratory under contract No. W-7405-Eng-48.

This report has been reproduced directly from the best available copy.

Available electronically at <http://www.doc.gov/bridge>
Available for a processing fee to U.S. Department of Energy
And its contractors in paper from
U.S. Department of Energy
Office of Scientific and Technical Information
P.O. Box 62
Oak Ridge, TN 37831-0062
Telephone: (865) 576-8401
Facsimile: (865) 576-5728
E-mail: reports@adonis.osti.gov

Available for the sale to the public from
U.S. Department of Commerce
National Technical Information Service
5285 Port Royal Road
Springfield, VA 22161
Telephone: (800) 553-6847
Facsimile: (703) 605-6900
E-mail: orders@ntis.fedworld.gov
Online ordering: <http://www.ntis.gov/ordering.htm>
Or
Lawrence Livermore National Laboratory
Technical Information Department's Digital Library
<http://www.llnl.gov/tid/Library.html>

Temporal incoherence induced upon a high-intensity beam by plasma propagation

J. Fuchs¹, C. Labaune¹, S. Depierreux², H. Bandulet¹, P. Michel¹, H.A. Baldis³

¹*Laboratoire pour l'Utilisation des Lasers Intenses, UMR n°7605 CNRS-École Polytechnique-CEA-Université Paris VI, École Polytechnique, 91128 Palaiseau Cedex, France*

²*CEA-DAM BIII, 91680 Bruyères Le Châtel, France*

³*Institute for Laser Science and Applications (ILSA), Lawrence Livermore National Laboratory, POB 808, Livermore, 94550 California, USA*

Abstract

Direct measurement of the coherence time of a high-intensity laser beam (600ps , 10^{14}W.cm^{-2}) after plasma propagation is achieved using a Michelson interferometer. Through plasma of interest for indirect-drive fusion ($0.1\times n_e$, 1 mm long), a large decrease of the coherence time is observed, from 100 ps to $\sim 10\text{ ps}$, induced by the interaction between the intense beam and the plasma. This decrease is even stronger as the light is scattered at larger angles from the initial beam angular distribution and as the plasma density is increased. The results coincide with trends observed in recent numerical simulations.

1 Introduction

For nearly two decades, much effort has been devoted to smooth out the far-field intensity distribution of the high-power lasers that are used for inertial confinement fusion (ICF) studies. To achieve such smoothing, several optical techniques to reduce the temporal and spatial coherence of the laser beams (random phase plates or RPP [1], smoothing by spectral dispersion or SSD [2], polarization smoothing [3], etc.) have been developed and implemented on the major ICF facilities [4]. The aim is to minimize, in time and space, the existence of undesirable hot spots that otherwise would be unavoidable due to the strong aberrations induced by high amplification of laser beams. Indeed, as these hot spots have intensities much higher than the average intensity, they have detrimental effects in laser-plasma interactions such as breaking the stringent irradiation uniformity required in ICF [5]. They also favor the growth of parametric instabilities and self-focus [6], leading to the reflection/scattering of a significant portion of the incoming laser light and further reducing the focal spot uniformity.

However, recent theoretical [7-9] and experimental [10-11] studies have shown that the coupling of the laser beams with the plasma along the propagation could strongly modify the coherence properties of the input laser. The underlying physics includes the resonant instability of individual filaments [8] that produces (i) self-phase modulation and spectral broadening through the fast density decrease within the filaments and (ii) a broad spectrum of scattered EM waves. This instability can trigger and enhance the non-linear coupling between self-focusing and forward stimulated Brillouin scattering [7] which in turn also broadens the scattered waves spectrum and sprays the energy at larger angles. Such induced incoherence has to be integrated in the predictive models for the NIF and LMJ performances as, on the one hand, it may angularly redistribute the energy and affect the irradiation symmetry but on the other hand, by reducing the coherence time and the speckle length [9], it may lower the growth of the parametric instabilities.

In this context, it is particularly important to quantify the effect of this induced smoothing as a function of the initial laser parameters. This is what we experimentally achieve by direct measurements of the laser coherence time in the output of the plasma. We show that it is strongly reduced and that such reduction depends on the laser initial intensity, plasma density and the angle at which the energy is scattered forward.

2 Experimental set-up and plasma conditions

The experiment is performed using four beams of the LULI (Laboratoire pour l'Utilisation des Lasers Intenses) laser facility. All beams are in the horizontal plane with 600 ps FWHM (full width at half maximum) Gaussian pulses, as illustrated in Fig.1. The plasma is formed by two counterpropagating, 526 nm wavelength laser beams incident on 380 μm diameter free-standing CH (parylene N) disks of thickness 1.2 μm , and heated by a third, identical beam, delayed by 0.5 ns with respect to the first two. These beams are propagated through RPPs (0.75 mm square elements) that produce a focal spot larger than the target.

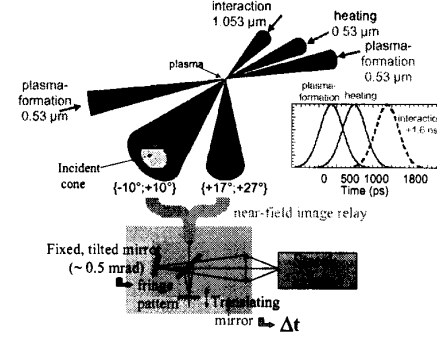


Fig.1: Experimental set-up. The forward scattered light of the interaction beam is collected into two cones, one on-axis, one off-axis. Either near-field plane can be sent into the Michelson interferometer.

The $\lambda=1.053 \mu\text{m}$ wavelength interaction beam is focused, through a 2 mm element RPP, with a $f/6$ optic along the principal axis of plasma expansion and delayed by 1.6 ns with respect to the plasma formation pulses. The focal spot diameter (at FWHM) is 320 μm , producing a peak average intensity of $\langle I_{\text{int}} \rangle \sim 1$ in units of 10^{14} W/cm^2 .

Plasma characterization has been extensively reported elsewhere [12]. Briefly, electron temperatures range between 0.5 and 0.7 keV during the interaction pulse. The electron density at the peak of the plasma profile decreases exponentially in time $n_{\text{top}}(t)/n_c \sim 0.13 \exp(-t[\text{ps}]/530)$ where $n_c = 1.1 \times 10^{21} \text{ cm}^{-3}$ is the critical electron density for $\lambda = 1.053 \mu\text{m}$ light and $t=0$ corresponding to the top of the interaction pulse. The typical scalelength of the inverse parabolic profile of the plasma is 700 μm . By lowering the energy of the plasma-formation beams, we also perform experiments using plasmas with a higher density, namely $n_{\text{top}}(t=0) \sim 0.6 \times n_c$.

The forward scattered light of the interaction beam is collected into two cones, one on-axis (having twice the aperture of the incident beam), one off-axis. This enables to study the coherence properties of the transmitted light from -10° to $+27^\circ$ from the axis of the incident interaction beam. For this purpose, several diagnostic stations are used.

For the direct measurement of the coherence time of the forward scattered light, the near-field in the collecting optics' plane is image-relayed onto the mirrors of a Michelson interferometer. The interferometer is set in an air-wedge configuration so as to produce a pattern of straight parallel fringes, localized on the mirrors' plane, over the whole field. This pattern is then imaged onto a streak camera whose slit (perpendicular to the fringes) selects only a part of the near-field. As each point in the near-field corresponds to a certain scattering angle, the slit position within the near-field image defines the angular range over which the coherence measurement is made. If the two arms of the interferometer are of equal length, the

two replicas of the pulse superimpose perfectly in time and perfect fringes should be observed at any time during the pulse evolution. However, if one arm is translated and a delay Δt is introduced between the two replicas, the fringes can become blurred if, during the pulse evolution, the light at time t is no more coherent with the light at time $t+\Delta t$. By scanning the delays, and by streaking the interference pattern for each delay, we can thus measure the coherence time of each moment within the temporal evolution of the pulse.

Complementarily, we measure the time-resolved spectra of the forward scattered light with spectral and temporal resolutions of 2 \AA and 150 ps respectively. This is done within the same angles as the ones used for the previous diagnostic, by imaging the transmitted far-field onto a spectrometer coupled to a streak camera. Moreover, insight into the correlated spatial coherence loss of the forward scattered light is obtained using 2D imaging of either the far-field or the near-field in the output of the plasma.

3 Results

3.1 Incident laser's temporal coherence

In order to be able to determine the influence of the propagation through the plasma on the temporal coherence of the laser, we first have to measure what the coherence time of the input laser is. This is achieved using the diagnostic station described above within the incident cone of the interaction beam and through vacuum. As shown in Fig.2.a, when the two arms of the Michelson interferometer are equal, we observe a fringe pattern with a good contrast $C \sim 0.9$ (as defined by $[I_{\max} - I_{\min}] / [I_{\max} + I_{\min}]$), constant over the entire pulse duration (the temporal resolution of the diagnostic is $\sim 30 \text{ ps}$). When we delay one replica within the interferometer by $\Delta t = 20 \text{ ps}$ (cf. Fig.2.b), we still observe clear fringes but with a slightly lower contrast. However, when the delay is increased to 100 ps , we observe in Fig.2.c that the fringes start to be blurred with a contrast near half of its value at $\Delta t = 0$, meaning that the coherence time of the incident laser is more than 100 ps if we

define, in the usual way, this value as the one at which $C = 0.5 \times C(\Delta t = 0)$. Note that the coherence time is the same from the beginning to the end of the pulse since the fringes' contrast remains constant during the pulse evolution.

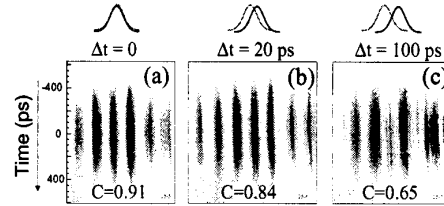


Fig.2: Measurement of the incident laser's coherence time. (a) Time-resolved fringe pattern within the incident cone at $\Delta t = 0$ – vacuum shot, (b) same but with $\Delta t = 20 \text{ ps}$, (c) same but with $\Delta t = 100 \text{ ps}$. The value of the pattern's contrast (C), constant during the pulse evolution, is given at the bottom of each image.

3.2 Modification of the temporal coherence after propagation through the plasma

When this beam is propagated at high-intensity ($\langle I_{\text{int}} \rangle \sim 1$) through the $\sim 0.1 \times n_c$, $\sim 1 \text{ mm}$ long plasma, its coherence time is greatly reduced, as shown in Fig.3. Here we select light that is scattered outside the incident cone, at $7 \pm 0.2^\circ$. Such scattering is due to the decrease of the spatial coherence, that was already observed in these conditions [11], which is evidenced by (i) the beam spreading at large angles and (ii) the spatial reduction of the filaments' size in the 2D images of the near-field. For $\Delta t = 2 \text{ ps}$ (cf. Fig.3.a), we observe very clear fringes with a good constant contrast (note that the fine structure within the dark fringes corresponds to spatial structures within the near-field scattered light and not to an interference effect). Strikingly, as soon as $\Delta t = 10 \text{ ps}$ (cf. Fig.3.b), we observe that the fringes, which are still clear

at the beginning of the pulse, are blurred around the temporal peak of the pulse and recover a good contrast only by the end of the pulse. This is clearly seen in the plot below Fig.3.b where the contrast of the fringes for the same image is measured as a function of time. This suggests that the blurring, or the temporal incoherence, is triggered by the high intensity part of the pulse since the low-intensity parts still keep a good fringe contrast. If we further increase the delay between the two replicas (cf. Fig.3.c), we see that the blurring is complete at the peak of the pulse. From these images, it is obvious that the coherence time of the laser is significantly modified by the propagation through the long, moderately dense plasma. More precisely, it decreases from more than 100 ps initially to less than 10 ps after plasma propagation.

Consistently, if we analyze this scattered light spectrally, it exhibits a strong broadening (up to 10 \AA) that appears, on the red side of the incident wavelength, around the peak of the pulse and slowly decreases in time to reduce to the incident linewidth by the end of the pulse, in agreement with what was observed previously [11]. Such spectral broadening is in excellent agreement with the direct measurement of the coherence time. Indeed the latter can be calculated [13] as $\tau = \lambda^2 / c \Delta\lambda$ ($\Delta\lambda$ being the FWHM spectral width). Here, as we measure $\Delta\lambda \sim 5 \text{ \AA}$ at the peak of the pulse, we get $\tau \sim 7 \text{ ps}$.

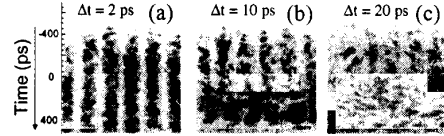


Fig.3: (a) time-resolved fringe pattern in the output of the Michelson interferometer after propagation at high-intensity ($I_{\text{in}} \sim 1$) through a $\sim 0.1 \text{ n/1 mm}$ plasma and with a delay $\Delta t = 2 \text{ ps}$ between the two replicas. Here $C \sim 0.5$ during all the pulse. (b) same with $\Delta t = 10 \text{ ps}$. At the bottom of the image, the evolution of the contrast (dots) during the pulse (dashed line) is given. (c) same with $\Delta t = 20 \text{ ps}$. Here, at the peak of the incident pulse, $C \sim 0.15$.

3.3 Dependence of the temporal coherence loss on the beam intensity, scattering angle and plasma density

In order to further confirm that the strong reduction of the coherence time of the laser is induced by the high intensity part within the laser pulse, we perform complementary measurements, in similar conditions as before and at $\Delta t = 10 \text{ ps}$, by lowering progressively the incident laser intensity. As observed in Fig.4, it is obvious that we finally recover clear fringes when the intensity is low enough.

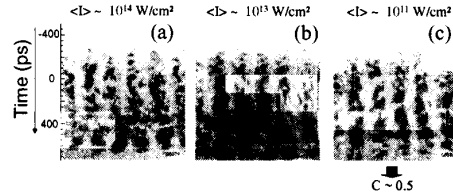


Fig.4: Fringe pattern measured in the same conditions as in Fig.3 but for varying incident intensity, namely $\langle I_{\text{in}} \rangle = 1$ in (a), 0.1 in (b) and 0.001 in (c).

To get more insight into the main physics involved in this process, we perform similar measurements but for light scattered at different angles. We observe that within the incident cone, the coherence time is longer ($\sim 15 \text{ ps}$) than the one slightly outside the cone that is shown in Fig.3. However, when we analyze the light scattered far outside the incident cone, at around 22° , the coherence time is then strongly reduced to $\sim 5 \text{ ps}$. Consistently, we observe that the spectrum of the light scattered at larger angles is also broader. It is interesting to note that this experimental trend is in concordance with what is observed in numerical simulations performed in close conditions [9]. The induced temporal incoherence is also favored by

increasing the plasma density. When the density at the peak of the pulse goes from $\sim 0.1 \times n_c$ to $\sim 0.6 \times n_c$, the fringe pattern at $\Delta t = 10$ ps starts blurring sooner and has a lower contrast than what can be seen in Fig.3.b. This is also consistent with the spectra recorded at high density. Indeed, here the red-shifted wing in the spectrum appears as soon as the pulse begins and stays on for the whole pulse duration. This behavior can be understood this way: when the plasma density is higher, the intensity needed to trigger the induced incoherence becomes lower, thus allowing the low-intensity parts of the pulse to have their coherence time reduced just like the high-intensity parts.

4 Summary

By direct measurement of the coherence time we have shown that the temporal coherence of a high-intensity laser beam is strongly reduced by propagation through a plasma whose parameters are of interest for indirect-drive ICF. The level of resulting temporal decorrelation is comparable with what can be achieved by SSD. This reduction is a non-linear phenomenon with a low threshold in intensity and increases with (i) the angle at which the energy is scattered forward and (ii) the plasma density. Obviously, such effect has to be taken into account in the smoothing strategies that will be implemented for the NIF or LMJ facilities.

Acknowledgments

The authors gratefully acknowledge the support of A. Michard and the technical groups of LULI. This work was performed under the auspices of the U.S. Department of Energy by University of California Lawrence Livermore National Laboratory, through the Institute for Laser Science and Applications, under contract No.W-7405-ENG-48.

References

- [1] Y. Kato *et al.*, *Phys. Rev. Lett.* **53**, 1057 (1984).
- [2] S. Skupsky *et al.*, *J. Appl. Phys.* **66**, 3456 (1989).
- [3] *LLE Review* **45** NTIS Document n° DOE/DP 40200-149 (1990).
- [4] A. Mostovych *et al.*, *Phys. Rev. Lett.* **59**, 1193 (1987); C. Labaune *et al.*, *Phys. Fluids B* **4**, 2224 (1992); W. Seka *et al.*, *Phys. Fluids B* **4**, 2232 (1992); B. McGowan *et al.*, *Phys. Plasmas* **3**, 2029 (1996); J. Fuchs *et al.*, *Phys. Rev. Lett.* **84**, 3089 (2000); J. Moody *et al.*, *Phys. Rev. Lett.* **86**, 2810 (2001).
- [5] J. Lindl, *Phys. Plasmas* **2**, 3933 (1995).
- [6] W. Kruer, *The physics of laser-plasma interactions*, Addison-Wesley, New-York (1988).
- [7] V. V. Eliseev *et al.*, *Phys. Plasmas* **4**, 4333 (1997); A. Schmitt and B. Afeyan, *Phys. Plasmas* **5**, 503 (1998).
- [8] D. Pesme *et al.*, *Phys. Rev. Lett.* **84**, 278 (2000).
- [9] A. Maximov *et al.*, *Phys. Plasmas* **8**, 1319 (2001).
- [10] J. Moody *et al.*, *Phys. Rev. Lett.* **83**, 1783 (1999); C. Labaune *et al.*, *C. R. Acad. Sci. Paris*, t.1, Série IV, 727 (2000).
- [11] J. Fuchs *et al.*, *Phys. Rev. Lett.* **86**, 432 (2001).
- [12] J. Fuchs *et al.*, *Phys. Plasmas* **7**, 4659 (2000).
- [13] M. Born and E. Wolf, *Principles of optics*, Pergamon Press, Oxford (1975) p.540.